

# Synthesis of Silica Encapsulated Perylenetetracarboxylic Diimide Core–Shell Nanoellipsoids

Hailin Wang,<sup>†</sup> Karola Schaefer,<sup>†</sup> Andrij Pich,<sup>\*,†,‡</sup> and Martin Moeller<sup>†,§</sup>

<sup>†</sup>DWI an der RWTH Aachen e.V., D-52056 Aachen, Germany

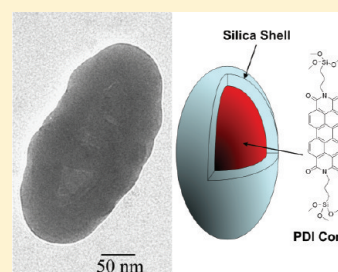
<sup>‡</sup>Functional and Interactive Polymers, Institute of Technical and Macromolecular Chemistry, RWTH Aachen University, D-52056 Aachen, Germany

<sup>§</sup>Textile Chemistry and Macromolecular Chemistry, Institute of Technical and Macromolecular Chemistry, RWTH Aachen University, D-52056 Aachen, Germany

 Supporting Information

**ABSTRACT:** Silica encapsulated perylenediimide (PDI) nanoellipsoids with core–shell structure have been synthesized in solution by a combination of precipitation method and sol–gel chemistry. Electron energy loss spectrum (EELS) analysis proves that the obtained composite particles consist of a PDI core and a silica shell. The UV–vis and fluorescence spectra show the strong  $\pi$ – $\pi$  stacking state of PDI molecules in the composite colloids. The silica deposition process on the PDI surface can be well controlled allowing variation of the shell thickness from 10 to 50 nm. Thermogravimetical analysis data indicate that the thermal stability of PDI increases after deposition of a silica shell. The photostability of PDI is enhanced by the introduction of silica shell. The silica coating improves the dispersibility of PDI in different solvents and in polymer films.

**KEYWORDS:** silica, perylene diimide, encapsulation, core–shell, nanoparticle



## INTRODUCTION

Perylenetetracarboxylic diimide (PDI) derivatives are an important class of functional dyes<sup>1</sup> and high performance pigments.<sup>2</sup> Because of their high photostability, chemical inertness, weather fastness, high color strength, and thermal stability, PDI pigments are widely used in the automotive paint and the coloration of synthetic fibers and resins. PDIs are also n-type semiconductors exhibiting relatively high electron affinity.<sup>3–5</sup> The research on the application of PDIs in electronic and optoelectronic devices, such as xerography<sup>3</sup> and dye-sensitized solar cell,<sup>6</sup> also draws great interests recently. Utilizing the strong fluorescence of PDIs, the application in imaging and bioanalysis<sup>7,8</sup> is also emerging.

Concerning the applications related to coloration where PDI is used as pigment, the design of particle size and morphology is critical.<sup>2</sup> One great challenge is to avoid the formation of large aggregates, which is crucial when high transparency is needed, for example for applications in optical devices. Small particles scatter light much less intensively than large ones; therefore, in the visible light range, transparent coatings can be prepared. Small particles are also easier to form stable dispersions, which is also very important for the application of pigments. Furthermore, particles with smaller size are also easier to form close packed film on a substrate and to improve the fastness. However, the structure of PDI determines that the molecules tend to form a strong  $\pi$ – $\pi$  stacking state, which means that PDI has a tendency to form large aggregates.

One possibility is the bottom-up procedure for fabrication of PDI colloids. Among numbers of available techniques, self-assembly

in solutions is a practical method to achieve ordered architectures.<sup>9–11</sup> The self-organization of PDI derivatives in solution holds strong interest for the present research on PDI,<sup>12–14</sup> especially on unsymmetrical substituted PDI.<sup>15–18</sup> Up to now, the self-assembly of PDI into nanobelts,<sup>15</sup> hollow vesicles,<sup>16</sup> nanofibers,<sup>17–19</sup> and microtubes<sup>20</sup> has been reported. At the same time, the preparation of PDI core–shell particles also attracts great attention.<sup>7,8,21</sup> The combination of bottom-up assembly with surface modification realizes the control of size and size distribution and at the same time improves compatibility with different materials.

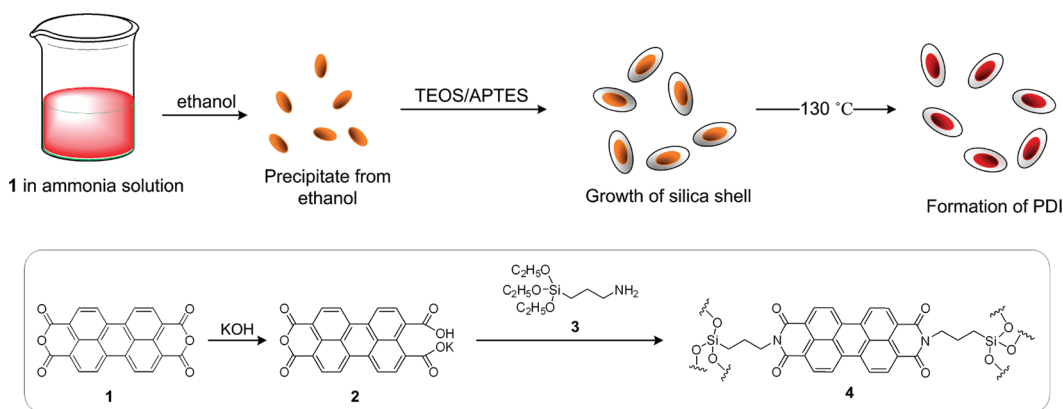
Silica is a widely used encapsulation material.<sup>22</sup> Silica as a host processes many advantages over traditional organic or inorganic materials. Silica is inert, highly transparent, dielectric material. Silica is resistant to many chemical attacks, stable in most environments, nontoxic, and biocompatible. Silica particles can be prepared with very small size. The surface modification and functionalization of silica is well established.<sup>23</sup> The surface property of silica can be tailored from hydrophilic to hydrophobic to suit different applications. Polymerization can also be performed on the surface of silica for improved affinity of silica to polymer.<sup>8</sup> Therefore, silica is a very suitable host which can be doped with different structures and functionalities, introducing various properties to the materials as a whole. Silica nanoparticles have been used to incorporate dye molecules by physical adsorption

**Received:** June 17, 2011

**Revised:** September 18, 2011

**Published:** October 06, 2011

Scheme 1. Synthesis Procedure of Silica Encapsulated PDI Nanoellipsoids



and chemical binding.<sup>24–28</sup> Utilizing these techniques, PDI doped silica nanoparticles<sup>8,21</sup> and mesoporous films<sup>29</sup> have been reported.

Here, we present a convenient liquid phase method that can fabricate silica coated PDI nanoellipsoids with core–shell structures. The deposition of silica on the surface of PDI stabilizes the PDI assemblies and prevents them from further growth and agglomeration. Through controlling the reaction process, the thickness of the silica shell and the morphology of these particles can also be controlled. Our results show that the silica coating increases the photostability and thermal stability of PDI. The dispersibility of the PDI particles is also improved by the silica shell. Moreover, the silica shell makes further modification and functionalization possible by using functional silanes.

## EXPERIMENTAL SECTION

**Synthesis of Perylene-3,4,9,10-tetracarboxylic Acid Monoanhydride Monopotassium.** A mixture of 3.92 g of 3,4,9,10-perylenetetracarboxylic dianhydride (0.01 mol, 97%, Aldrich) and 5.0 g of KOH (0.09 mol, pellet, for analysis, Merck) in 100 mL of water was heated to 90 °C and kept at this temperature for 4 h. The red solid was hydrolyzed and dissolved in water gradually. The solution turned to orange with green fluorescence. The solution was filtered to remove unreacted solids and adjust the pH to 4.0 with 10 wt % H<sub>3</sub>PO<sub>4</sub> (crystalline, ≥99.999%, Aldrich) solution. Red precipitate appeared. The red solid was filtered and washed with water. Then, the product was dried at 60 °C.

**Synthesis of Silica Coated PDI Core–Shell Nanoellipsoids.** In a typical procedure,  $2 \times 10^{-5}$  mol of perylene-3,4,9,10-tetracarboxylic acid monoanhydride monopotassium was dissolved in 1.8 mL of 25% ammonia aqueous solution (KMF). A transparent orange solution with strong green fluorescence was formed. This solution was added to 18 mL of absolute ethanol (VWR) with vigorous stirring. Afterward, 1 mmol of tetraethyl orthosilicate (TEOS, reagent grade, 98%, Aldrich) and 0.25 mmol of 3-aminopropyltriethoxysilane (APTES, ≥98%, Sigma-Aldrich) were added as precursors of silica. This dispersion was kept for 12 h under gentle stirring for the growth of silica. Then, the particles were transferred to diethylene glycol (DEG, ≥99.0%, Sigma-Aldrich) and heated to 130 °C for three hours. After having been cooled to room temperature, these particles were separated by centrifugation and washed with water and ethanol. Very fine red powders were obtained. Then, these particles were dispersed in water for further characterization.

### Octadecyl-Modification of Silica Coated PDI Core–Shell Nanoellipsoids.

To make the silica coated PDI particles hydrophobic, the synthesized nanoellipsoids in the previous step were dispersed in 100 mL of ethanol. And then, 0.1 mL of octadecyltrimethoxysilane (technical grade, 90%, Aldrich) in 2 mL of ethanol was added to the particle dispersion with vigorous stirring. Afterward, 0.5 mL of 25% ammonia solution was added. The dispersion was allowed to keep 24 h under stirring at room temperature. The particles were isolated by centrifugation. Then the particles were washed several times with toluene and ethanol to remove excess silanes and then were redispersed in toluene.

### Synthesis of Bis(propyl) Triethoxysilane Perylenediimide.

Bis(propyl) triethoxysilane perylenediimide (PDI-BPTES) is prepared according to the literature.<sup>20</sup> Briefly, a portion of 0.392 g (1 mmol) of 3,4,9,10-perylenetetracarboxylic dianhydride and 1 mL of APTES were added into a flask. The flask was repeatedly evacuated and flushed with nitrogen. The mixture was stirred for 5 min, then heated to 130 °C, and held for 3 h. After cooling to room temperature, the mixture was washed with hexane to remove excess APTES. Then acetone was used to extract the residues. The solvent was evaporated, and the product was collected to give a red powder of bis(propyl) triethoxysilane perylenediimide. <sup>1</sup>H NMR (400 MHz, CDCl<sub>3</sub>, TMS,  $\delta_H$ , ppm): 8.42 (4H, d, Ar–H), 8.24 (4H, d, Ar–H), 4.18 (4H, t, N–CH<sub>2</sub>), 3.84 (12H, q, O–CH<sub>2</sub>), 1.87 (4H, m, N–CH<sub>2</sub>CH<sub>2</sub>), 1.25 (18H, t, O–CH<sub>2</sub>CH<sub>3</sub>), 0.78 (4H, t, Si–CH<sub>2</sub>). <sup>13</sup>C NMR: (100 MHz, CDCl<sub>3</sub>, TMS,  $\delta_C$ , ppm): 163.97 (C=O), 134.00, 130.96, 128.92, 125.85, 123.10, 122.71, 58.47 (OCH<sub>2</sub>), 43.72 (N–CH<sub>2</sub>), 21.43 (N–CH<sub>2</sub>CH<sub>2</sub>), 18.34 (OCH<sub>2</sub>CH<sub>3</sub>), 8.08 (Si–CH<sub>2</sub>). FTIR (KBr,  $\bar{\nu}_{max}$ , cm<sup>−1</sup>): 3434, 2972 (–CH<sub>3</sub>), 2926 (–CH<sub>2</sub>–), 2883 (–CH<sub>2</sub>–), 1696 (–CO–N–CO–), 1656 (–CO–N–CO–), 1595 (Ar), 1578 (Ar), 1344, 1102, 1077, 1018 (Si–C), 810 (Si–C), 745 (–(CH<sub>2</sub>)<sub>3</sub>–).

**Preparation of Polymer Film Containing Silica Coated PDI Particles.** A solvent casting procedure was used to prepare the composite films. A 10 wt % poly(vinylpyrrolidone) (PVP,  $M_w$  = 10000, Sigma-Aldrich) ethanol or water solution containing silica coated PDI particles (5 wt % of PVP) is applied onto a flat glass slide without imposing hydrodynamic stress on the liquid. The solvent was allowed to evaporate under ambient conditions until the film hardened.

**Characterization.** Transmission electron microscope (TEM) and electron energy loss spectrum (EELS) measurements were performed by a Zeiss Libra 120 (Carl Zeiss, Oberkochen) EFTEM equipped with LaB<sub>6</sub> filament and an in-column OMEGA filter. The electron beam accelerating voltage was set at 120 kV. The sample was first suspended in ethanol by ultrasonic treatment for 20 min. A drop of this well-dispersed suspension was then trickled on a piece of carbon-coated copper grid. Before being placed into the TEM specimen holder, the copper grid was

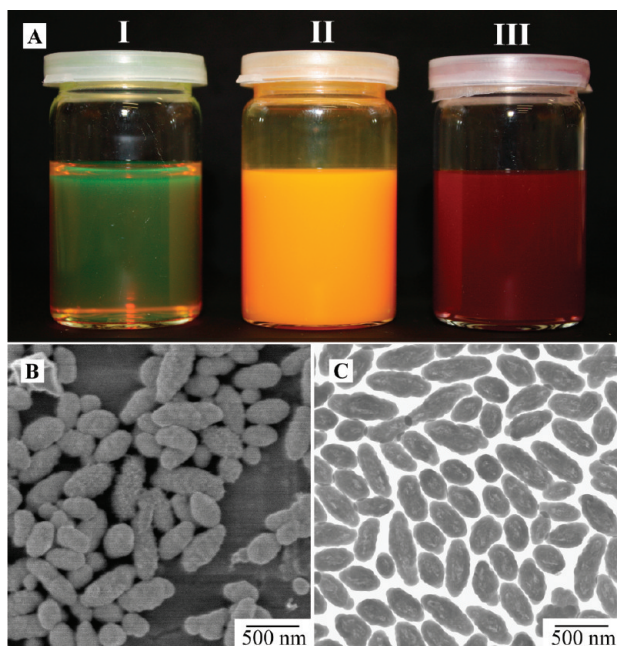


**Figure 1.** (A) Photograph of perylene salt **1** in aqueous ammonia solution (I), the dispersion formed by addition of **I** into ethanol (II), and the ethanol dispersion of the final product silica coated PDI (III); FESEM (B) and TEM (C) image of the silica coated PDI particles.

air-dried under ambient conditions. The EELS spectra and elemental mapping were processed by the software WinTEML. Field emission scanning electron microscope (FESEM) measurements were performed on a Hitachi S-4800 FESEM. Infrared (IR) spectra were obtained by a Nicolet 60 SXR FT-IR spectrometer using PAS or KBr methods.  $^1\text{H}$ - and  $^{13}\text{C}$ -liquid nuclear magnetic resonance (NMR) spectra were recorded on a Varian Inova 400 MHz spectrometer at room temperature. Tetramethylsilane (TMS) was used as an internal standard. UV-vis spectra were measured with the help of a Varian Cary 100 UV-vis spectrophotometer. Fluorescent spectra were measured by a Perkin Elmer LS-50 photoluminescence spectrometer. The polymer film was characterized by Zeiss Axioplan 2 microscope under dark field mode. Thermogravimetric analysis (TGA) was performed on a NETZSCH TG 209c unit operating under a nitrogen atmosphere with a flow rate of  $10\text{ mL}\cdot\text{min}^{-1}$ . The samples were dried at  $120\text{ }^\circ\text{C}$  for 6 h to remove solvents before measurements. Then 10–15 mg of sample was measured in a standard NETZSCH alumina  $85\text{ }\mu\text{L}$  crucible. For photobleaching measurement, samples of silica coated PDI nanoellipsoids and PDI-BPTES were continuously irradiated and examined by a Zeiss Axioplan 2 fluorescence microscope equipped with XBO 75 illuminating system (Xenon lamp) using a filter using a filter  $\lambda_{\text{ex}} \geq 470\text{ nm}$  and  $\lambda_{\text{em}} \geq 500\text{ nm}$ . Images were acquired every 10 min. The images were analyzed by the software ImageJ to obtain the intensity of the fluorescence. For each sample, three data sets, representing different fields of view, were averaged and then normalized to the same initial fluorescence intensity value to facilitate comparison.

## RESULTS AND DISCUSSION

**Synthesis of Silica-Coated PDI Nanoellipsoids.** The synthetic strategy developed in present study is outlined in Scheme 1. Perylene-3,4,9,10-tetracarboxylic acid dianhydride (**1**) is used as the precursor for PDI. After **1** is hydrolyzed in KOH aqueous solution, perylene-3,4,9,10-tetracarboxylic acid monoanhydride monopotassium (**2**) is obtained.<sup>30</sup> In a typical procedure,

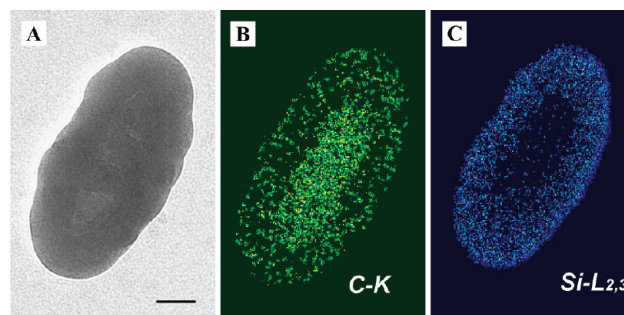


**Figure 2.** Bright field TEM image of one single silica encapsulated PDI particle (A) and the elemental maps of the same particle: (B) C-K elemental map, (C) Si-L<sub>2,3</sub> elemental map (the bar represents 50 nm).

$2 \times 10^{-5}$  mol potassium salt **2** was dissolved in 1.8 mL of 25% ammonia aqueous solution, and a transparent orange solution (**I**) showing strong green fluorescence was formed (Figure 1A, I). The solution was then added to 18 mL of ethanol with vigorous stirring. The perylene salt is insoluble in ethanol and precipitates from the solution to form a yellow dispersion (**II**) (Figure 1A, II).

Afterward, 1 mmol of tetraethyl orthosilicate (TEOS) and 0.25 mmol of 3-aminopropyltriethoxysilane (APTES, **3**) were added as precursors of silica. This dispersion was kept for 12 h under gentle stirring for the growth of silica shell. The color of the dispersion changed slightly from yellow to orange. In order to stabilize the perylene in silica, the particles were then transferred to diethylene glycol which has a higher boiling point than ethanol, and the dispersion was heated at  $130\text{ }^\circ\text{C}$  for 3 h. The amino group of APTES reacted with the perylene salt to produce silsesquioxane substituted PDI **4**.<sup>20</sup> Therefore, the perylene is converted to PDI after being incorporated in the silica matrix. During this step, the color quickly changed from orange to dark red upon heating (Figure 1A, III). After cooling to room temperature, the solid was separated from the dispersion by centrifugation and washed with ethanol and water. No color and fluorescence was observed in the supernatant. The product can be well dispersed in water and ethanol. The dispersion keeps stable for months.

**Morphology of Composite Particles.** Field emission scanning electron microscopy (FESEM) and transmission electron microscopy (TEM) were used to study the surface morphology and internal structure of core-shell particles. The FESEM and TEM (Figure 1B and C) images show that almost all the particles have ellipsoidal shape. The particle length and width vary from 80 to 400 nm and from 40 to 60 nm, respectively. The surface of the particles is not very smooth. The TEM images reveal that all particles have an inhomogeneous composition. The outer layer of the particle shows a different contrast compared with the center of the particle, which indicates that the particle has core-shell structure. The particle should be composed by a less dense core and a 20–50 nm thick shell made of relatively denser material.

To investigate the internal structure of the particles, energy-filtered TEM (EFTEM) was employed for image electron energy loss spectroscopy (EELS) measurement, which provides information about the localized elemental distribution with very high resolution.<sup>31</sup> Figure 2 depicts the C-K elemental map and Si-L<sub>2,3</sub> elemental map of single nanoellipsoid particle. It is clear that silicon is mainly located in the outer layer of the particle, while the center contains a much higher concentration of carbon. This confirms the core-shell structure of the particle.



The Fourier transform infrared (FTIR) spectrum of the particle is shown in Figure 3. As a comparison, the spectra of silica and PDI are also presented. The peaks at 1696, 1656, and 1596  $\text{cm}^{-1}$  indicate the presence of imide groups. The strong peak at 1074  $\text{cm}^{-1}$  confirms the existence of silica. Therefore, it can be concluded that the particle is composed of a layer of silica outside and PDI core inside. Thus, the contrast difference of the particle's different parts on TEM images can also be explained because silica gives higher contrast than PDI on bright field TEM image. Because APTES is condensed together with TEOS to form silica, carbon also exists in the outer layer but with a much lower concentration than in the center.

**Optical Properties of Composite Particles.** The absorption and fluorescence spectra were used to monitor the process of forming PDI assembly. The dilute solution of perylene salts **2** in water shows strong green fluorescence with emission maxima at  $\lambda_{\text{em}} = 479 \text{ nm}$  and  $\lambda_{\text{em}} = 510 \text{ nm}$  (Figure 4). Upon addition of ethanol to the solution, an absorption band appears at around 525 nm, and the absorption in longer wavelength increases,

which indicates the formation of  $\pi$ – $\pi$  stacking state of the PDI molecules.<sup>15,32</sup>

After heating, the absorption below 525 nm was strongly decreased and the absorption at longer wavelength was enhanced (Figure 4A) because of the formation of extended  $\pi$ – $\pi$  stacking aggregates. The green emission ( $\lambda_{\text{em}} = 482$  and 510 nm) of the ethanol dispersion **II** of perylene salts (Figure 4B b) indicates the unorganized state of the molecules when the aggregates initially are formed. The final product (Figure 4B c), however, shows red emission ( $\lambda_{\text{em}} = 633 \text{ nm}$ ), which is well-known for  $\pi$ -stacked PDI.<sup>33</sup> The red shift in emission suggests a highly ordered state and strong intermolecular interactions.<sup>33</sup>

Because fluorescence emission spectra are sensitive to the solvent polarity,<sup>8,34</sup> we studied the fluorescence of the prepared silica coated PDI particles in different solvents. The results (Figure 5) show that the emission at around 630 nm has no obvious shift in polar solvents (ethanol and water) and nonpolar solvents (toluene, after the particles have been hydrophobized by octadecyl group). This suggests that the PDI is in similar environments when the particles are dispersed in water, ethanol, and toluene, which indicates the PDI has no direct contact with the solvents. Therefore, the silica shell provides a quite good protection for the PDI core.

**Influence of Reaction Parameters on Particle Size and Morphology.** The nature of PDI is critical for the formation of the core–shell structure in present system. The reaction mixture contains ethanol, ammonia, and TEOS, which is similar to the Stöber system for the preparation of monodisperse spherical silica nanoparticles.<sup>35</sup> However, in our synthesis, almost all the particles have core–shell structure, and no pure silica or uncoated PDI nanoellipsoids were found. This implies a strong interaction between silica and PDI. When the aqueous ammonia solution of perylene salts **2** is added to ethanol, the salt precipitates from the solution and aggregates are formed because of the low solubility in ethanol. These aggregates have ellipsoidal shape (Supporting Information Figure S2). It is known that perylene derivatives have a relative high electron affinity.<sup>3,4</sup> Therefore, the concentration of  $\text{OH}^-$  ions might be higher around the aggregates. The  $\text{OH}^-$  ion is the catalyst for the hydrolysis and condensation of TEOS and APTES.<sup>23</sup> Also considering the

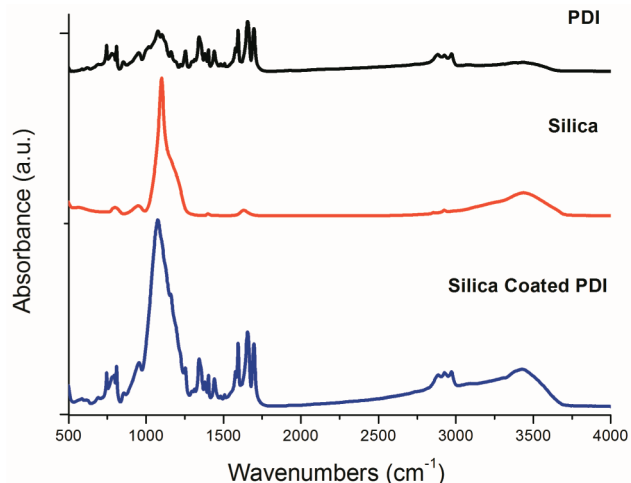


Figure 3. FTIR spectra of PDI, silica, and the silica coated PDI particles.

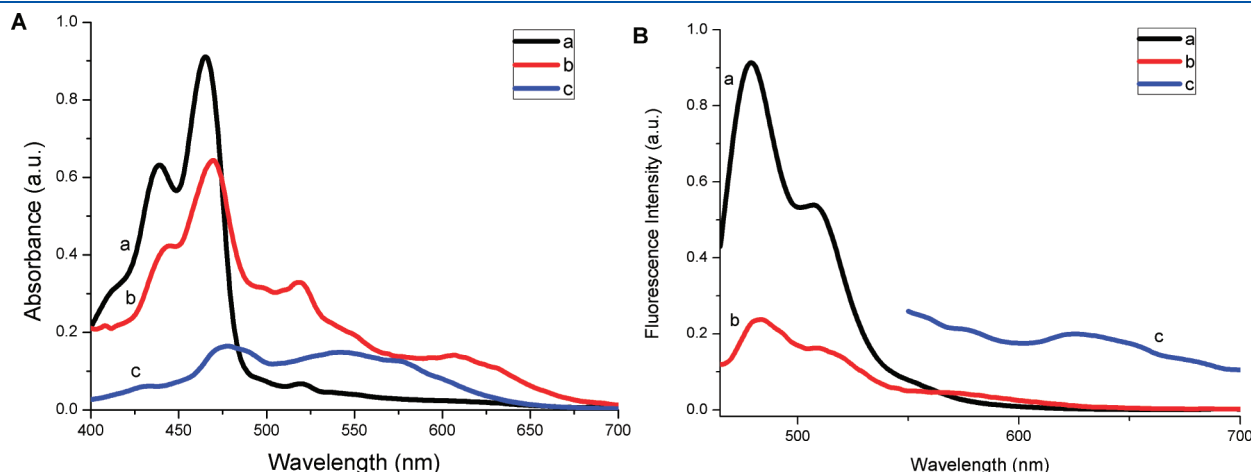
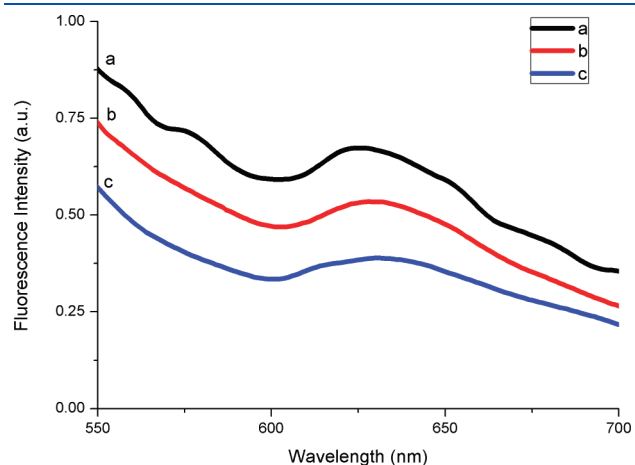


Figure 4. Absorption (A) and fluorescence emission (B) spectra of dilute aqueous solution **I** (a), the dispersion **II** in ethanol formed by adding the solution **I** to ethanol (b) and the ethanol dispersion of the final product of silica encapsulated PDI particles (c). The excitation wavelength is 465 nm (a), 460 nm (b), and 486 nm (c), respectively. The emission spectrum of c is only shown from 550 nm because the scattering light from the silica coated particles is too strong (see Supporting Information Figure S1 for the spectrum from 500 nm).

hydrogen bonding between the Si—OH and PDI, the nucleation and growth of silica may be preferable on the surface of PDI aggregates. The deposition of silica on the surface of PDI prevents the PDI aggregates from further growth and agglomeration. Upon addition of TEOS and APTES the morphology of the particle does not change obviously, except that a layer of silica grows uniformly on the PDI surface.

The concentration of ammonia has a significant impact on the morphology and structure of the silica coated PDI particles. On the one hand, the precursor of PDI is dissolved in ammonia



**Figure 5.** Fluorescence emission spectra of silica encapsulated PDI particles dispersed in ethanol (a: excited at 486 nm), water (b: excited at 491 nm), and octadecyl-modified silica encapsulated PDI particles dispersed in toluene (c: excited at 472 nm).

solution. The concentration of ammonia has influence on the precipitation of PDI in ethanol. On the other hand, as in Stöber synthesis, the ammonia is the catalyst which controls the hydrolysis and condensation of TEOS and ultimately the size of the particles. In the typical synthetic procedure discussed above, an optimized ammonia concentration of 1.2 M is used. If the ammonia concentration is as low as 0.33 M, no PDI-silica core-shell particles can be prepared. Only irregular PDI aggregates and separate silica structures were observed (Figure 6A). When the concentration of ammonia increases to 0.67 M, silica coated PDI ellipsoids were obtained but with a thinner silica shell, and isolated silica nanoparticles were also observed (Figure 6B). When ammonia concentration reaches 2.0 M, silica coated PDI ellipsoids were prepared, and no isolated silica particles could be observed (Figure 6C, D). However, the appearance of the shell is quite different from that of particles prepared in the typical procedure. The surface of the shell is very rough and fluctuant. Hemispherical structures can be observed on many parts of the shell.

At low ammonia concentration, like in the Stöber synthesis, more silica nuclei form and the reaction is slower, and maybe the surface of PDI does not have so high affinity to silica at lower pH. Therefore, the formation of silica will not be limited on the PDI surface. Ultimately, free silica particles appear, and a thinner shell is obtained. When the ammonia concentration is too low, there is not enough ammonia for the formation of stable primary silica particles, and consequently no core-shell structure will be prepared. At high ammonia concentration, the formation of silica is faster, and the PDI surface has higher affinity to silica. Hence, the deposition of silica on the PDI surface is so rapid that the silica intends to form spheres on the surface similar as in the

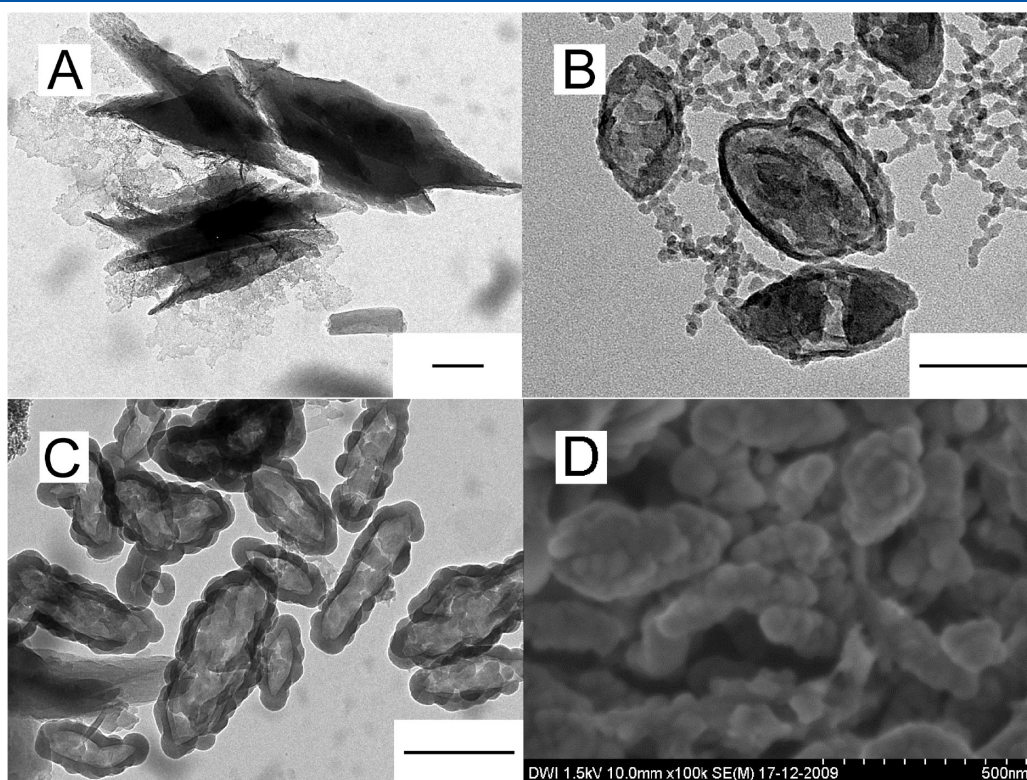


**Figure 6.** TEM (A, B, C) and FESEM (D) images of silica coated PDI particles prepared at ammonia concentration of (A) 0.33 M, (B) 0.67 M, and (C, D) 2.0 M. The scale bar in TEM image represents 250 nm.

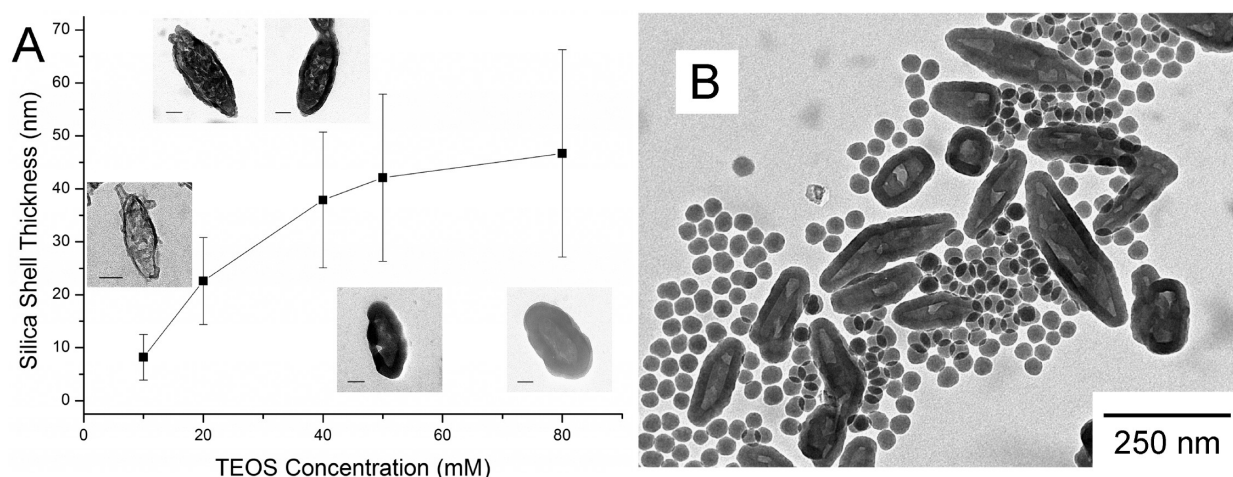


**Figure 7.** The variation of the silica shell thickness with TEOS concentration (the insets are the TEM images of corresponding particles, scale bars 50 nm) (A); TEM image of silica coated PDI nanoellipsoids prepared at high TEOS concentration (0.2 M) (B).

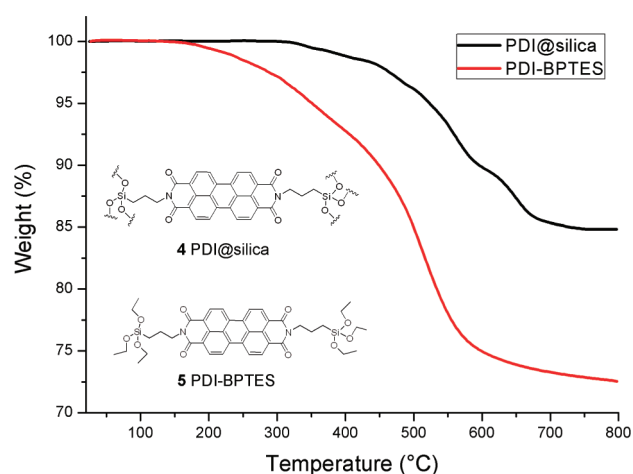


**Figure 8.** TGA curves of silica coated PDI nanoellipsoid (PDI@silica) and bis(propyl) triethoxysilane perylene diimide (PDI-BPTES) under nitrogen atmosphere and 10 K/min heating rate.

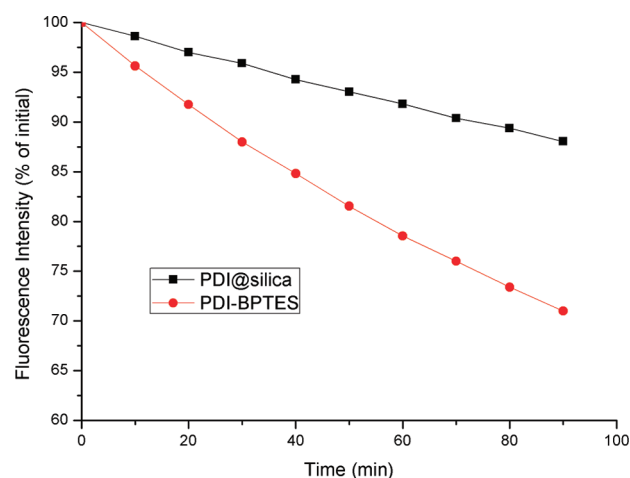


**Figure 9.** Photobleaching profile of PDI@silica particles and PDI-BPTES obtained by continuous illumination of the sample under a fluorescence microscope equipped with a Xe lamp using a filter  $\lambda_{\text{ex}} \geq 470$  nm and  $\lambda_{\text{em}} \geq 500$  nm.

Stöber synthesis. This is the reason why surfaces with many hemispheres are observed.

The concentration of TEOS in reaction mixture has less influence on the morphology of the formation of core-shell particles compared to ammonia. However, the thickness of the shell can be controlled by the TEOS concentration. In a certain range, the thickness of the shell increases with an increase of the TEOS concentration (Figure 7A). When the concentration of TEOS is greater than 0.1 M, isolated silica spherical particles appear (Figure 7B). In the case of high concentration of TEOS, the concentration of silicic acid in the system becomes so high that the nucleation is very fast. Therefore, the PDI surface cannot provide enough area for the nucleation and growth of silica. Hence, spherical silica nanoparticles also form beside the silica shell on PDI. However, a thicker silica shell still can be prepared by adding TEOS in a step-by-step manner.

Due to the fact that PDI nanoparticles after the precipitation step continue growing in solution, the delayed addition of silica precursors TEOS and APTES led to the formation of core-shell particles with different morphologies. For example, if TEOS

and APTES were added after 1 h when the solution of perylene salt 2 was added to ethanol, the PDI particles became larger and exhibited a rod-like shape. The resulting core-shell particle also has similar rod morphology (Supporting Information Figure S3). If the solution was kept at 60 °C before the addition of TEOS and APTES for 1 h, then nanosheets with hexagonal shape can be prepared (Supporting Information Figure S4). If the reaction was kept standing without stirring, the aggregates grew longer to ribbon-like morphology, and tube-like core-shell particles were obtained (Supporting Information Figure S5).

**Thermal Stability of Composite Particles.** Perylene pigments are thermally stable. However, in some cases higher temperatures are required especially during incorporation of pigments in polymer blends by melt extrusion. In order to investigate the influence of silica coating on the thermal stability of PDI, we studied the thermal decomposition of the prepared silica coated PDI nanoellipsoids by thermogravimetric analysis (TGA). As a comparison, bis(propyl) triethoxysilane perylene diimide (5, PDI-BPTES, Figure 8) was also studied which has



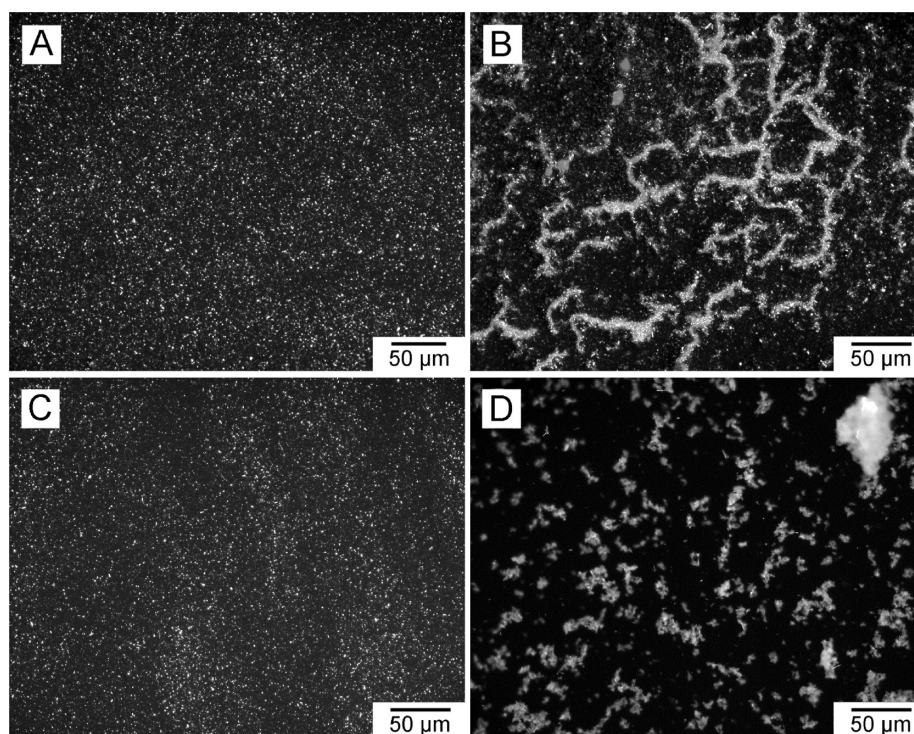


**Figure 10.** Dark field optical microscope images of PVP film containing silica coated PDI (A and C) and PDI without silica coating (B and D). (A and B): films obtained after casting from ethanol solution; (C and D): films obtained after casting from aqueous solution.

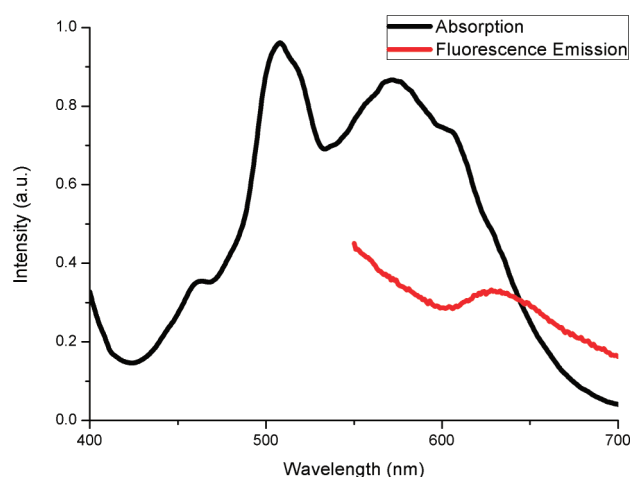


**Figure 11.** Absorption and fluorescence emission spectra of PVP film with incorporated silica coated PDI particles.

the structure of noncross-linked PDI parts in silica coated PDI particles. The TGA curves are shown in Figure 8. The decomposition of PDI is considered to be first initiated with the degradation of alkyl substituents. Generally, the longer alkyl and branched alkyl substituted compounds show lower decomposition temperatures.<sup>36</sup> In this study, the decomposition rate of PDI@silica is much slower than that of the PDI-BPTES. The onset temperature of thermal decomposition is 432 °C for PDI-BPTES and 495 °C for PDI@silica. Obviously, the thermal stability of PDI can be significantly improved by the silica coating and cross-linking.

**Photostability of Composite Particles.** To study the influence of silica shell on the photostability of PDI, the photobleaching

of PDI fluorescence under continuous irradiation was investigated. After 90 min of illumination by Xe lamp, the fluorescence intensity of silica encapsulated PDI particles drops to around 88% of the initial intensity. As a comparison, the value for PDI-BPTES is 71% (Figure 9). This implies that the existence of silica shell protects the PDI from quenchers such as oxygen and improves the photostability.

#### Incorporation of Composite Particles in Polymer Films.

The deposition of silica shell on the surface of PDI nanoellipsoids prevents the composite particles from forming large aggregates and improves the dispersibility in different media. This is a great advantage for the preparation of stable PDI dispersions or composite polymer films filled with PDI. After the PDI is coated with silica, the dispersibility of pigments is only related to the interface chemistry of silica rather than to PDI itself. As the surface chemistry of silica has been thoroughly studied and can be finely tuned, the dispersibility of silica coated PDI particles can also be controlled in order to suit for different matrices.

Here, as a simple example to verify the performance of the core-shell PDI nanoellipsoids, we prepared poly(vinylpyrrolidone) (PVP) films containing PDI particles with or without silica shell. Figure 10 (A and B) shows the dark field optical microscope images of the PVP films prepared by PVP ethanol and water solution containing dispersed PDI particles, respectively. The bright dots in the images are the PDI particles. For both films prepared in ethanol and water, the silica coated PDI particles are almost homogeneously distributed throughout the whole film and no large aggregates can be found. The absorption and fluorescence emission spectra of the PVP film containing silica encapsulated PDI particles are also recorded (Figure 11) which are quite similar with the spectra of particles in ethanol dispersion (Figure 4). This also indicates that these particles are well dispersed in the PVP films.

For comparison, we also used PDI particles without silica shell which are prepared by the same procedure as silica coated PDI particles but without the use of TEOS and APTES. The results show that these particles form large aggregates and agglomerates in the film rather than distribute homogeneously (Figure 10 B and D).

## CONCLUSION

In this work, we developed a solution-based method for preparation of silica coated PDI core-shell nanoellipsoids. The structure and composition of the particles was proved by FTIR and image EELS. The absorption and fluorescence spectra show strong  $\pi$ - $\pi$  stacking of the PDI molecules. The morphology of the particle and the thickness of the silica shell can be controlled through variation of the experimental conditions. The increase of the TEOS concentration in the reaction mixture from 10 mM to 80 mM induces an increase of the silica shell thickness from 10 to 40 nm. The increase of the ammonia concentration accelerates the growth of the silica shell. However, at high ammonia concentrations the shell around PDI cores is formed from discrete silica nanoparticles probably due to the very fast nucleation process. This increases the surface roughness of the silica shell on the PDI nanoellipsoid surface considerably. Based on these experimental data we proposed the mechanism of the shell formation. The silica coating can significantly improve the thermal stability of the PDI nanoellipsoids. TGA experimental data indicate the shift of decomposition temperature by 70 °C to higher values. Additionally, the photostability and the dispersibility in polymer films of the silica coated PDI were improved.

## ASSOCIATED CONTENT

**Supporting Information.** The full fluorescence emission spectrum of silica encapsulated PDI nanoellipsoids and TEM images of uncoated PDI and PDI-silica composited prepared at different addition modes of TEOS and APTES. This material is available free of charge via the Internet at <http://pubs.acs.org>.

## AUTHOR INFORMATION

### Corresponding Author

\*Phone: +49 (0)241 80 233 50. Fax: +49 (0)241 80 233 01.  
E-mail: [pich@dw.rwth-aachen.de](mailto:pich@dw.rwth-aachen.de).

## ACKNOWLEDGMENT

We wish to thank the research associations Dechema Gesellschaft für Chemische Technik und Biotechnologie e.V., Frankfurt a. M./D and Forschungskuratorium Textil e.V., Berlin/D, for the financial support of the research project IGF-No. 333 ZN, which is provided within the promotion program of "Industrielle Gemeinschaftsforschung und -entwicklung (IGF)" from budget funds of the Federal Ministry of Economics and Technology (BMWi) due to a resolution of the German Bundestag via Arbeitsgemeinschaft industrieller Forschungsvereinigungen e.V. A.P. is thankful for the funding of this research provided by Volkswagen Foundation.

## REFERENCES

- (1) Hunger, K. *Industrial Dyes: Chemistry, Properties, Applications*. Wiley-VCH: Weinheim, 2003.
- (2) Smith, H. M. *High Performance Pigments*. Wiley-VCH: Weinheim, 2002.

- (3) Law, K. Y. *Chem. Rev.* **1993**, 93, 449–486.
- (4) Newman, C. R.; Frisbie, C. D.; da Silva Filho, D. A.; Bredas, J.-L.; Ewbank, P. C.; Mann, K. R. *Chem. Mater.* **2004**, 16, 4436–4451.
- (5) Xu, B. Q.; Xiao, X. Y.; Yang, X.; Zang, L.; Tao, N. J. *J. Am. Chem. Soc.* **2005**, 127, 2386–2387.
- (6) Gregg, B. A. *J. Phys. Chem. B* **2003**, 107, 4688–4698.
- (7) Yin, M.; Shen, J.; Gropeanu, R.; Pflugfelder, G. O.; Weil, T.; Müllen, K. *Small* **2008**, 4, 894–898.
- (8) Ribeiro, T. N.; Baleizão, C.; Farinha, J. P. S. *J. Phys. Chem. C* **2009**, 113, 18082–18090.
- (9) Green, J. E.; Wook Choi, J.; Boukai, A.; Bunimovich, Y.; Johnston-Halperin, E.; DeIonno, E.; Luo, Y.; Sheriff, B. A.; Xu, K.; Shik Shin, Y.; Tseng, H.-R.; Stoddart, J. F.; Heath, J. R. *Nature* **2007**, 445, 414–417.
- (10) Hoebe, F. J. M.; Jonkheijm, P.; Meijer, E. W.; Schenning, A. P. H. J. *Chem. Rev.* **2005**, 105, 1491–1546.
- (11) Grimsdale, A. C.; Müllen, K. *Angew. Chem., Int. Ed.* **2005**, 44, 5592–5629.
- (12) Würthner, F.; Chen, Z.; Dehm, V.; Stepanenko, V. *Chem. Commun.* **2006**, 1188–1190.
- (13) Balakrishnan, K.; Datar, A.; Oitker, R.; Chen, H.; Zuo, J.; Zang, L. *J. Am. Chem. Soc.* **2005**, 127, 10496–10497.
- (14) van Herikhuyzen, J.; Syamakumari, A.; Schenning, A. P. H. J.; Meijer, E. W. *J. Am. Chem. Soc.* **2004**, 126, 10021–10027.
- (15) Che, Y.; Datar, A.; Balakrishnan, K.; Zang, L. *J. Am. Chem. Soc.* **2007**, 129, 7234–7235.
- (16) Zhang, X.; Chen, Z.; Würthner, F. *J. Am. Chem. Soc.* **2007**, 129, 4886–4887.
- (17) Yang, X.; Xu, X.; Ji, H.-F. *J. Phys. Chem. B* **2008**, 112, 7196–7202.
- (18) Everett, T. A.; Twite, A. A.; Xie, A.; Battina, S. K.; Hua, D. H.; Higgins, D. A. *Chem. Mater.* **2006**, 18, 5937–5943.
- (19) Yan, P.; Chowdhury, A.; Holman, M. W.; Adams, D. M. *J. Phys. Chem. B* **2005**, 109, 724–730.
- (20) Luo, Y.; Lin, J.; Duan, H.; Zhang, J.; Lin, C. *Chem. Mater.* **2005**, 17, 2234–2236.
- (21) Blechinger, J.; Herrmann, R.; Kiener, D.; García-García, F. J.; Scheu, C.; Reller, A.; Bräuchle, C. *Small* **2010**, 6, 2427–2435.
- (22) Bergna, H. E.; Roberts, W. O. *Colloidal Silica: Fundamentals and Applications*. CRC: Boca Raton, 2006; Vol. 131.
- (23) Iler, R. K. *The Chemistry of Silica: Solubility, Polymerization, Colloid and Surface Properties and Biochemistry of Silica*. Wiley: New York, 1979.
- (24) Larson, D. R.; Ow, H.; Vishwasrao, H. D.; Heikal, A. A.; Wiesner, U.; Webb, W. W. *Chem. Mater.* **2008**, 20, 2677–2684.
- (25) Bagwe, R. P.; Yang, C.; Hilliard, L. R.; Tan, W. *Langmuir* **2004**, 20, 8336–8342.
- (26) Van Blaaderen, A.; Vrij, A. *Langmuir* **1992**, 8, 2921–2931.
- (27) Montalti, M.; Prodi, L.; Zaccheroni, N.; Falini, G. *J. Am. Chem. Soc.* **2002**, 124, 13540–13546.
- (28) Rampazzo, E.; Bonacchi, S.; Montalti, M.; Prodi, L.; Zaccheroni, N. *J. Am. Chem. Soc.* **2007**, 129, 14251–14256.
- (29) Feng, J.; Liang, B.; Wang, D.; Wu, H.; Xue, L.; Li, X. *Langmuir* **2008**, 24, 11209–11215.
- (30) Tröster, H. *Dyes Pigm.* **1983**, 4, 171–177.
- (31) Hofer, F.; Grogger, W.; Kothleitner, G.; Warbichler, P. *Ultra-microscopy* **1997**, 67, 83–103.
- (32) Würthner, F. *Chem. Commun.* **2004**, 1564–1579.
- (33) Liu, S.-G.; Sui, G.; Cormier, R. A.; Leblanc, R. M.; Gregg, B. A. *J. Phys. Chem. B* **2002**, 106, 1307–1315.
- (34) Lakowicz, J. R. *Principles of Fluorescence Spectroscopy*, 3rd ed.; Springer: US, 2006.
- (35) Stober, W.; Fink, A.; Bohn, E. *J. Colloid Interface Sci.* **1968**, 26, 62–69.
- (36) Nagao, Y. *Prog. Org. Coat.* **1997**, 31, 43–49.